JOC The Journal of Organic Chemistry

Article

pubs.acs.org/joc

Stable 5,5′-Substituted 2,2′-Bipyrroles: Building Blocks for Macrocyclic and Materials Chemistry

Gonzalo Anguera,[†] Brice Kauffmann,[§] José I. Borrell,[‡] Salvador Borrós,[†,⊥] and David Sánchez-García*[,†]

[†]Grup d'Enginyeria de Materials (GEMAT), Institut Químic de Sarrià, Universitat Ramon Llull, Via Augusta, 390, Barcelona 08017, Spain

[‡]Grup d'Enginyeria Molecular, Institut Químic de Sarrià, Universitat Ramon Llull, Via Augusta, 390, Barcelona 08017, Spain

[§]Institut Européen de Chimie et Biologie, Université de Bordeaux-CNRS UMS3033, INSERM US001, Rue Robert Escarpit, 33607 Pessac, France

[⊥]Centro de Investigación Biomédica en Red en Bioingeniería, Biomateriales y Nanomedicina (CIBER-BBN), Zaragoza 50018, Spain

Supporting Information

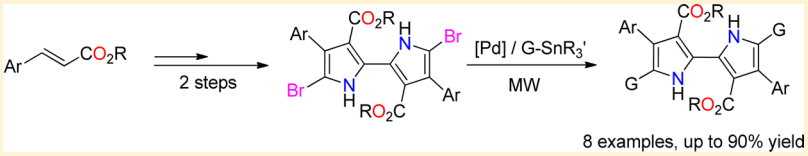

ABSTRACT: The preparation and characterization of a family of stable 2,2′-bipyrroles substituted at positions 5 and 5′ with thienyl, phenyl, TMS-ethynyl, and vinyl groups is reported herein. The synthesis of these new bipyrroles comprises three steps: formation of the corresponding 5,5′-unsubstituted bipyrrole, bromination, and Stille or Suzuki coupling. The best results in the coupling are obtained using the Stille reaction under microwave irradiation. The new compounds have been fully characterized by UV−vis absorption, fluorescence, and IR spectroscopies and cyclic voltammetry. X-ray single-crystal analysis of four of the synthesized bipyrroles indicates a trans coplanar geometry of the pyrrole rings. Furthermore, the substituents at positions 5,5′ remain coplanar to the central rings. This particular geometry extends the π-conjugation of the systems, which is in agreement with a red-shifting observed for the λ_{max} of the substituted molecules compared to the unsubstituted bipyrrole. All of these new compounds display a moderate fluorescence. In contrast with unsubstituted bipyrroles, these bipyrroles are endowed with a high chemical and thermal stability and solubility in organic solvents.

INTRODUCTION

Our initial interest in 2,2′-bipyrroles[1] stems from their presence as structural motifs in relevant natural products, such as prodigiosin[2] or vitamin B_{12}.[3] However, in recent years, the development of the chemistry of 2,2′-bipyrroles has been focused on their application as building blocks for the preparation of artificial porphyrinoids,[4] for instance, porphycenes,[5] sapphyrins,[6] or cyclo[8]pyrroles.[7] More recently, the availability of such bipyrroles has spurred their use as monomers for the preparation of conjugated polymers.[8−12] Unfortunately, the synthesis of 2,2′-bipyrroles and especially β,β′-substituted bipyrroles still entails long synthetic pathways and leads to chemically unstable products, such as α,α′-free bipyrroles **1** (Figure 1).[13−16] This instability hampers the functionalization of the α-position of the pyrrole rings, thus limiting the application of these compounds.

In 2009, our group developed a new family of 2,2′-bipyrroles **2** bearing two ester functionalities at the β positions of pyrroles starting from cinnamates (Figure 1).[17] In contrast to the α,α′-free bipyrroles **1**, bipyrroles **2** exhibit a high stability and can be stored indefinitely in the fridge. The chemical stability of bipyrroles **2** was rationalized in terms of a decrease in the charge density of the pyrrolic nucleus by the esters. Encouraged by the stability of these bipyrroles, the synthesis of a substituted

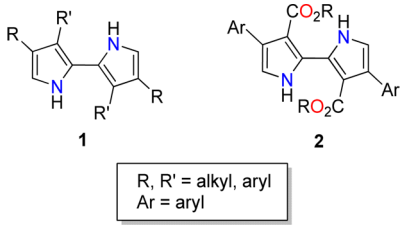

Figure 1. β,β′-Substituted bipyrroles **1** and **2**.

quaterpyrrole was envisaged by a double-Suzuki coupling between an α,α′-dibrominated bipyrrole and *N*-Boc-2-pyrroleboronic acid.[18] The successful preparation of such a quaterpyrrole prompted us to generalize this synthetic methodology, giving a straightforward access to substituted bipyrroles **3** bearing aromatic and unsaturated moieties at positions 5,5′ (Scheme 1). The conjugated structure and the presence of the bipyrrolic moiety make these new molecules of interest in the design of metal ligands,[19−23] macrocyclic receptors,[4,22,24−27] molecular electronics,[28] light-emitting diodes,[29] electrochromic devices,[10] molecular wires,[30] the

Received: May 2, 2017
Published: May 26, 2017

DOI: 10.1021/acs.joc.7b00961
J. Org. Chem. 2017, 82, 6904−6912

Scheme 1. Synthesis of 2,2′-Bipyrroles 3a−h

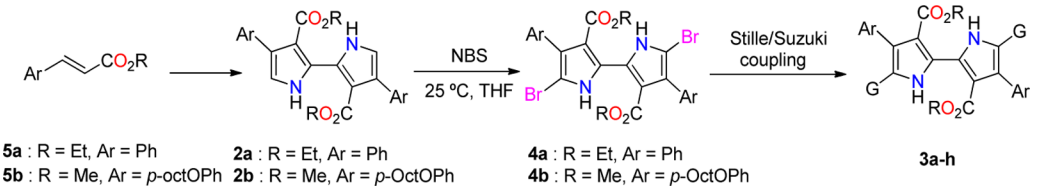

Table 1. Functionalization of Brominated 2,2′-Bipyrroles 4a,b Using Stille and Suzuki Reactions under Microwave Irradiation

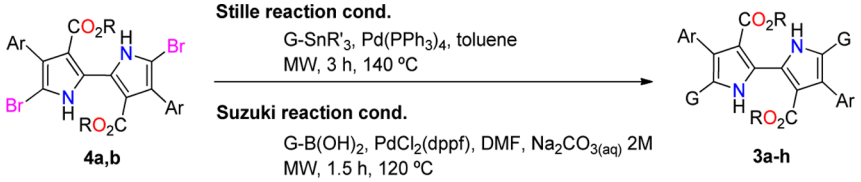

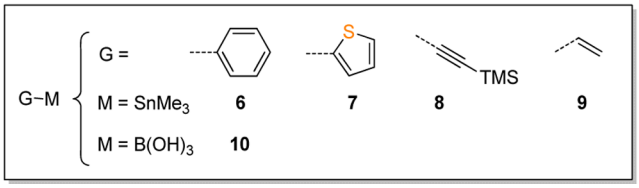

entry	R	Ar	G	M	method	product	yield (%)
1	Et	Ph	2-thienyl	$SnBu_3$	Stille	**3a**	87
2	Et	Ph	Ph	$SnMe_3$	Stille	**3b**	90
3	Et	Ph	Ph	$B(OH)_2$	Suzuki	**3b**	35
4	Et	Ph	TMS-ethynyl	$SnBu_3$	Stille	**3c**	79
5	Et	Ph	vinyl	$SnBu_3$	Stille	**3d**	63
6	Me	4-(octyloxy)Ph	2-thienyl	$SnBu_3$	Stille	**3e**	90
7	Me	4-(octyloxy)Ph	Ph	$SnMe_3$	Stille	**3f**	92
8	Me	4-(octyloxy)Ph	TMS-ethynyl	$SnBu_3$	Stille	**3g**	32
9	Me	4-(octyloxy)Ph	vinyl	$SnBu_3$	Stille	**3h**	46

preparation of conjugated low band gap polymers,[31−34] and polymer-based sensors.[35−39]

Thus, herein the synthesis of substituted bipyrroles **3** is reported. The optical properties (UV−vis and fluorescence), electrochemistry (cyclic voltammetry), and thermal stability of these new molecules have been studied. These results have been rationalized with the aid of DFT and TD-DFT computations. The molecular structures of some selected bipyrroles have been revealed by single-crystal X-ray diffraction.

RESULTS AND DISCUSSION

Synthesis. In this work, positions 5,5′ of bipyrroles **2a,b** are substituted by means of palladium-catalyzed reactions, namely Stille and Suzuki couplings.[40] The starting materials for such couplings are the corresponding dibrominated bipyrroles **4a,b**, which are prepared by exposure of α,α'-free bipyrroles **2a,b** to 2 equiv of NBS.[18] Bipyrroles **2a,b** are accessible from cinnamates **5a,b** following a one-pot, two-step process reaction previously reported by our group (Scheme 1).[17]

The nature of the substituents at the β positions of bipyrroles is given by the choice of the starting cinnamate. Their presence is quite convenient, enhancing solubility and the chemical stability to the bipyrrole moiety. Furthermore, the ester groups can be easily removed under specific conditions.[33] For the sake of simplicity, in this work, methyl and ethyl cinamates have been used as starting materials. Two different aromatic moieties have been chosen: the phenyl group and the *p*-OctOPh.

The synthesis of bipyrroles **2a,b** is based on our previously reported methodology.[17] First, *p*-toluenesulfonylmethyl isocyanide (TOSMIC) ester was treated with 2 equiv of *n*-BuLi and 2 equiv of trimethyltin chloride ($SnMe_3Cl$) at −78 °C. Then the corresponding cinnamate **5a,b** was added to render a stannylated pyrrole intermediate that was, in turn, treated with an excess of $Cu(NO_3)_2{\cdot}3H_2O$ to afford 4,4′-diaryl-2,2′-bipyrroles **2a,b** by oxidative dimerization. This one-pot, two-step process furnished bipyrroles **2a,b** in moderate yields (42% and 27%, respectively). Next, the bromination of bipyrroles was carried out by treatment of **2a,b** with *N*-bromosuccinimide in THF as solvent at room temperature.[18] Both brominated bipyrroles **4a,b** were obtained in good yields (87% and 75%, respectively).

Once the brominated bipyrroles were in hand, preparation of substituted bipyrroles **3** was attempted by Stille and Suzuki cross-coupling reactions. Preliminary experiments were carried out by refluxing bipyrrole **4a** with reagents **6** and **10** under typical conditions used to perform such couplings (Table 1).[41] Although the couplings were successfully achieved, long reaction times (12 and 48 h for Suzuki and Stille couplings, respectively) were needed to reach good conversions. To simplify the preparation, conventional heating was advantageously replaced by microwave irradiation (MW).[42,43] Under these conditions, the reaction time was reduced significantly (1.5 and 3 h for Suzuki and Stille couplings, respectively) while affording the corresponding products in similar yields.

DOI: 10.1021/acs.joc.7b00961
J. Org. Chem. 2017, 82, 6904−6912

Table 2. Crystal Data and Structure Refinements for compounds 2a, 3a, 3b, and 3f[a]

compd	2a	3a	3b	3f
formula	$C_{52}H_{48}N_4O_8$	$C_{34}H_{28}N_2O_4S_2$	$C_{38}H_{32}N_2O_4$	$C_{52}H_{60}N_2O_6$
formula wt	856.94	592.70	580.65	809.02
T (K)	120	100	120	120
wavelength (Å)	1.54178	1.54178	1.54178	1.54178
space group	$P21/n$	P-1	P-1	$P21/n$
a (Å)	8.1443(16)	8.282 (6)	8.1568 (1)	13.109 (3)
b (Å)	18.723(4)	9.706 (9)	10.0681 (6)	10.350 (2)
c (Å)	14.403(3)	10.928 (7)	11.061 (4)	16.408 (3)
α (deg)	90	113.515 (11)	63.31 (3)	90
β (deg)	98.79(3)	93.064 (1)	68.71 (3)	94.59 (3)
γ (deg)	90	114.23(3)	66.74 (3)	90
V	2170.4 (8)	709.4 (9)	724.0 (3)	2219.1 (8)
Z/D_{calcd} (g/cm^3)	2/1.311	1/1.387	1/1.332	2/1.211
$F(000)$	904	310	306	868
μ (mm^{-1})	0.722	2.01	0.69	0.595
h, k, l_{max}	9, 22, 17	9, 11, 13	9, 12, 13	15, 12, 20
T_{min}/T_{max}	0.960, 1.000	0.875, 1.000	0.929, 1.000	0.959, 1.000
S	1.04	1.118	1.172	1.044
R_1(reflns)	0.0334 (3830)	0.0451 (2282)	0.0566 (2357)	0.0505 (3711)
wR_2 (reflns)	0.0866 (4075)	0.1264 (2539)	0.1545 (2570)	0.1412 (4211)

[a] $R_1 = \sum||F_o| - |F_c||/\sum|F_o|$, $wR_2 = [\sum[w(F_o^2 - F_c^2)^2]/\sum[w(F_o^2)^2]]^{1/2}$.

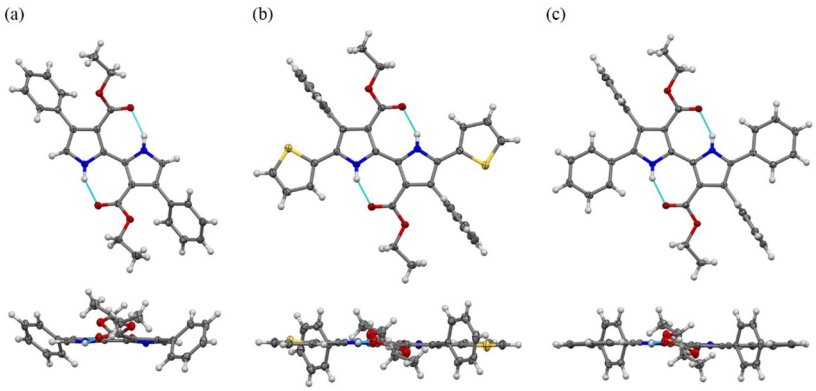

Figure 2. X-ray crystal structures of bipyrroles **2a** (a), **3a** (b), and **3b** (c). Displacement ellipsoids are shown at the 50% probability level.

Although both reactions provide the coupling products, generally, the Stille reaction affords the products in higher yields than the Suzuki coupling (Table 1, entries 2 and 3). This result might be ascribed to the hydrolysis of the ester groups at positions 3,3′ of the bipyrrolic moiety due to the basic conditions or the dehalogenation of position 5,5′.[44] Therefore, the Stille coupling was adopted to prepare a small library of substituted bipyrroles.

The workup of the reaction was straightforward and was carried out by simple washings of the crude solids with mixtures of ethyl acetate and cyclohexane. All synthesized products were characterized by ^{1}H, ^{13}C NMR, infrared spectroscopy, and elemental analysis (EA). The results of such analyses clearly demonstrate the purity and structure of the compounds. The yields of the 5,5′-substituted bipyrroles **3** are in the range of 32−92% (Table 1).

X-ray Crystal Structure Analysis. Single crystals suitable for X-ray analysis for bipyrroles **2a**, **3a**, **3b**, and **3f** were obtained from slow evaporation of mixtures of $CHCl_3$/AcOEt or by slow diffusion of cyclohexane into chloroform solutions of the compounds (Table 2). Figure 2 shows the ORTEP plots of **2a** and **3a**,**b** with thermal ellipsoids at the 50% probability level.

The structure of bipyrrole **3f** is shown in the Supporting Information (SI) (Figure S16). In all of the substituted bipyrroles (**3a**, **3b**, and **3f**), the central two pyrrole rings are found to adopt the same coplanar and *trans* configuration (dihedral angles between −0.7(4)° and −2.2(6)°). Interestingly, the structure of unsubstituted bipyrrole **2b** shows a slight deviation from planarity, being the corresponding dihedral angle −11.0(2)°. In general, this planarity is a consequence of the two hydrogen bonds formed between carbonyl groups and the hydrogens from each pyrrolic unit. The bond distances for these hydrogen bonds are in the range of 1.808−1.925 Å (Figure 2). This geometry would allow a high π-conjugation of the molecules, which is in agreement with the spectroscopic data. In fact, the bond distances between sp^2-carbon atoms at positions 2 and 2′ (∼1.45 Å) are shorter than the typical C−C bond, implying a partial double-bond character.

The phenyl groups at positions 4,4′ are twisted with respect to the plane of the 2,2′-bipyrrole moiety, making a dihedral angle in the range of 59.3(2)° and 99.8(3)°. In contrast, the rings at positions 5,5′ adopt an almost planar geometry. Thus, for the phenyl groups the dihedral angle is 4.3(5)°, whereas the thiophene moieties are only slightly out of the plane

DOI: 10.1021/acs.joc.7b00961
J. Org. Chem. 2017, 82, 6904−6912

(−1.7(4)°). In compound **3a**, the thiophene and pyrrole rings adopt a *trans* conformation.

The crystal-packing views of these bipyrroles are shown in the Supporting Information (SI) (Figures S17−S19) and in Figure 3. In the solid state, bipyrrole **2a** is packed in a

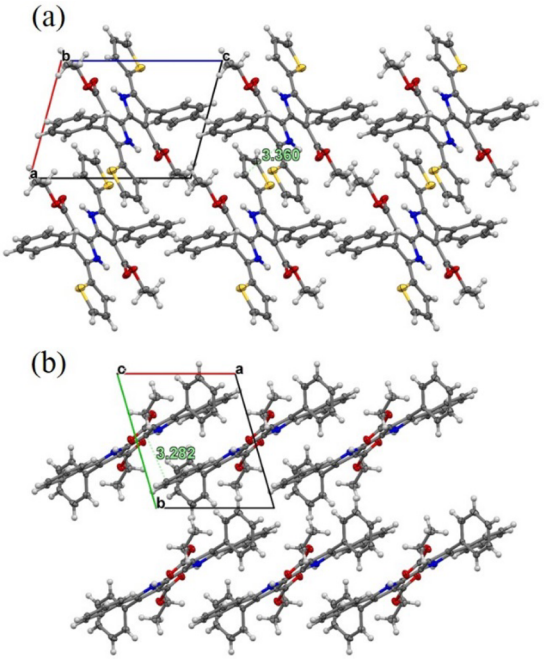

Figure 3. X-ray crystal packing of bipyrrole **3a** (a) (along crystallographic *b* axis) and **3b** (b) (along crystallographic *c* axis).

herringbone fashion with an interlayer distance of 3.2 Å (Figure S17). An intermolecular CO−π interaction is observed between the ester group and the pyrrole ring (Figure S18).[45] The introduction of thiophene and phenyl rings at positions 5,5′ leads to the formation of supramolecular linear arrangements stabilized by π−π stacking between one pyrrole and the adjacent ring of two near bipyrroles. The π−π stacking distances are around 3.3 Å (Figure 3). Interestingly, in bipyrrole **3f** the bulkiness of the octyl chains hampers any π−π stacking interactions (Figure S19).

Thermal Stability. Pyrroles and oligopyrroles are generally regarded as chemically unstable and prone to oxidation.[11] Thus, in order to assess the applicability of the bipyrroles of this study in optoelectronics, it is critical to evaluate their thermal stability.[46] To do so, thermogravimetric analyses (TGA) were performed on four bipyrroles (**2a** and **3a**−**c**) (Figure 4). Compound **3d** was not studied due to the intrinsic instability of the vinyl groups. Interestingly, the data showed that all products are unaltered below 230 °C. Additionally, the parameter T_{d10} (10% loss mass) was found to range from 285 °C (**3a**) to 339 °C (**3b**).

Electronic Absorption Spectroscopy. The UV−vis absorption spectra of bipyrroles **2**, **3**, and **4** were measured in chloroform solution (Figure 5a and Figures S20−S25). The corresponding spectral data are summarized in Table 3. The common feature of these spectra is the presence of a moderately strong absorption band (16000−24000 $cm^{-1}\cdot M^{-1}$) around 400 nm, which is the λ_{max}^{abs}. This characteristic band corresponds to $\pi \rightarrow \pi^*$ transitions between adjacent heterocycles. As a general trend, the longest λ_{max}^{abs} values of the substituted compounds are notably red-shifted as compared to

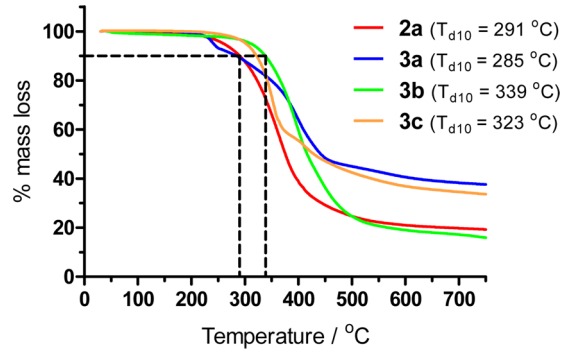

Figure 4. Thermograms for 2,2′-bipyrroles **2a** and **3a**−**c** and T_{d10}.

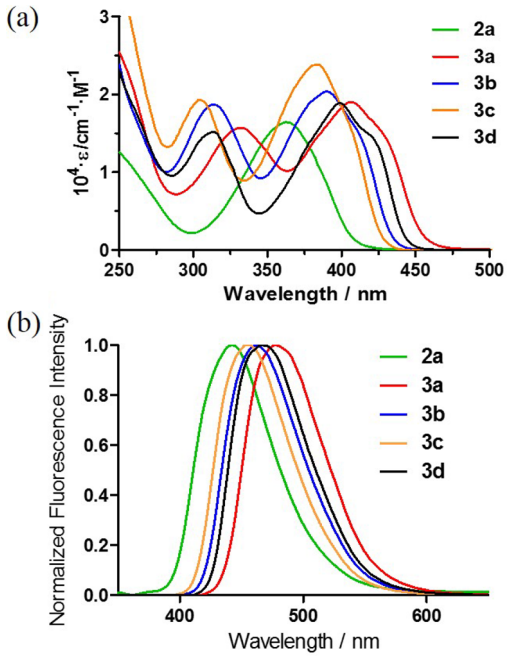

Figure 5. UV−vis absorption spectra (a) and normalized fluorescence emission excited at their maximum absorption wavelength (b) of **2a** and **3a**−**d**.

Table 3. UV-vis Absorption and Fluorescence Properties of 2a,b, 4a,b, and 3a−h

	absorption				fluorescence	
product	λ_{max1} (nm)	λ_{max2} (nm)	ε_{max1}	ε_{max2}	λ (nm)	Φ
2a	362		16000		443	0.78
4a	372		20000		446	0.55
3a	406	332	19000	16000	477	0.23
3b	390	314	20000	19000	462	0.52
3c	383	305	24000	19000	454	0.73
3d	399	313	19000	16000	466	0.49
2b	368		21000		451	0.77
4b	376		22000		453	0.31
3e	408	334	22000	18000	485	0.23
3f	392	314	21000	19000	468	0.49
3g	387	301	21000	17000	461	0.62
3h	403	313	19000	16000	473	0.4

the value displayed by bipyrrole **2a**. This effect is rationalized in terms of the extension of the π-conjugation of the molecules.

DOI: 10.1021/acs.joc.7b00961
J. Org. Chem. 2017, 82, 6904−6912

Furthermore, when the 5,5′ positions of the bipyrrole unit are substituted with unsaturated moieties, an additional absorption band emerges in the 320 nm region. In accordance with the TD-DFT calculations (Table 5), these high-energy bands are mainly attributed to electronic transitions among the pyrrolic moiety and the unsaturated groups at positions 5,5′ (Figure S36).

As expected, the *p*-octyl chain in the phenyl present in the 4,4′ position does not produce noticeable effects on the absorption spectrum; in most cases, only a bathochromic shift of 2−6 nm was observed.

Fluorescence Spectroscopy. The fluorescence spectra of bipyrroles **2**, **3**, and **4** in chloroform are shown in Figure 5b and Figures S20−S25. The spectral data are summarized in Table 3. Typically, 2,2′-bipyrroles display strong fluorescence emissions observed above 440 nm with high quantum yields (Figure 5).[47] For instance, the 5,5′-unsubstituted bipyrrole **2a** displays a fluorescence peak at 443 nm with a luminescence quantum yield of 78%. The introduction of the trimethylsilylethynyl, phenyl, vinyl, and thiophene groups onto positions 5,5′ causes a significant red-shifting of the maximum of the emission band, accompanied by a gradual decrease in the quantum yield from 73% (**3c**) to 23% (**3a**). This effect is especially dramatic in the case of compound **3a**. The introduction of two thiophene rings causes a red-shift of 34 nm compared with **2a**, and the quantum yield is reduced to 23% (Figure 6). On the other hand, in bipyrroles **3c** and **3g** the introduction of the trimethylsilylethynyl moiety only slightly reduces the emission. Again, the presence of the *p*-octyl chain does not significantly change the fluorescence parameters.

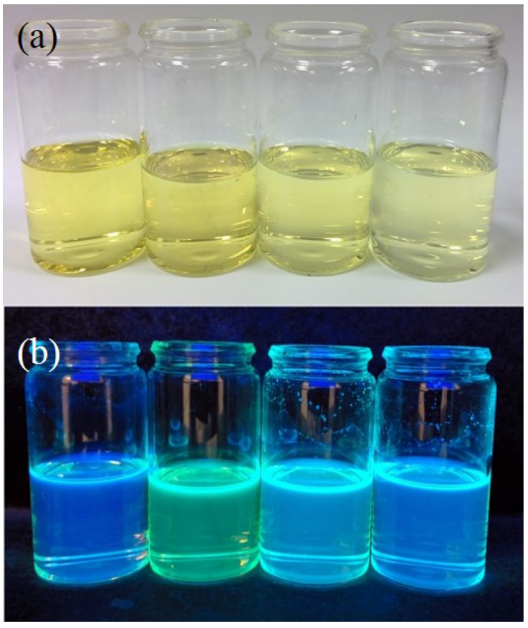

Figure 6. Photographs of chloroform solutions of **2a** and **3a−c** (a) and their fluorescence emission exited at 330 nm (b).

Electrochemical Properties. With the aim of elucidating the electronic effects of the introduction of substituents onto position 5,5′ of the bipyrrole moiety of bipyrroles **5**, their electrochemical behavior was examined by cyclic voltammetry (CV) (Figures S26−S30). The measurements were performed in deoxygenated dichloromethane (0.5 mM) containing 0.1 M *n*-Bu_4NClO_4 (TBAP) as a supporting electrolyte. All potentials reported herein were calibrated with the ferrocene/ferrocenium couple (Fc/Fc^+) as internal standard. The oxidation potentials (E_o) and onsets (E_{ox}^{onset}) of **2a** and **3a−d** are listed in Table 4. The onset potential was measured relative to the Fc/Fc^+ couple. The energy level of Fc/Fc^+ was assumed to be −4.80 eV relative to the vacuum level.[48]

α,*α*′-Unsubstituted bipyrrole **2a** and bipyrroles **3c**,**d** display one oxidation peak at around 0.5 V (Table 4). The first oxidation wave can be attributed to the formation of a radical cation species.[49] In contrast, thiophene (**3a**) and 5,5′-diphenyl (**3b**) substituted bipyrroles show two reversible oxidation waves (Figure 7). Interestingly, the values of the oxidation potentials

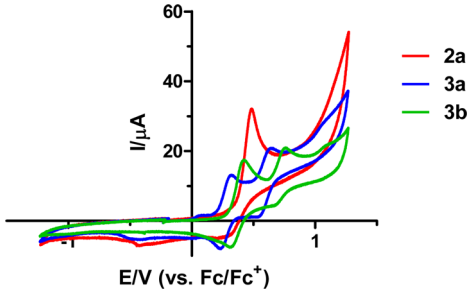

Figure 7. Cyclic voltammetry for bipyrroles **2a** and **3a**,**b**.

for bipyrrole **3a** are cathodically shifted by ca. 100 mV in comparison with the phenyl-containing bipyrrole **3b**. This enhancement of the donor ability of compound **3a** is accounted for the high conjugation of the molecule, which is in agreement with the UV−vis data and the electrochemical features of related terpyrroles and quaterpyrroles.[49,50] On the basis of the onset potential of their first oxidation waves, the HOMO energy levels for bipyrroles **2a** and **3a−d** were estimated to be −5.09, −4.91, −5.02, −5.20, and −4.97 eV, respectively (Table 4).

Theoretical Calculations. DFT calculations were performed using the Becke's three-parameter hybrid functional and gradient-corrected correlation functional of Lee.[51,52] First, the geometries were optimized at the B3LYP/6-311G (d,p) level.

Table 4. Electrochemical Data and HOMO−LUMO Band Gaps of Bipyrroles 2a and 3a−d

compd	E_o[a] (V)	E_{ox}^{onset}[b] (V)	E_{HOMO}^{exp}[c] (eV)	E_{HOMO}^{calcd}[d] (eV)	E_{LUMO}^{exp}[e] (eV)	E_g^{opt}[f] (eV)	E_g^{calcd}[g] (eV)
2a	+0.47	+0.29	−5.09	−5.39	−2.06	3.03	3.32
3a	+0.29	+0.11	−4.91	−4.99	−2.02	2.71	2.98
3b	+0.40	+0.22	−5.02	−5.11	−2.16	2.86	3.22
3c	+0.58	+0.40	−5.20	−5.29	−2.30	2.90	3.30
3d	+0.4	+0.17	−4.97	−5.15	−2.17	2.80	3.07

[a] E_o, first oxidation peak potential; [b] E_{ox}^{onset}, onset oxidation potential; [c] $E_{HOMO}^{exp} = -(E_{ox}^{onset}+4,8)$. [d] E_{HOMO}^{calcd}, calculated by B3LYP/6-311G(d,p)//B3LYP/6-311G(d,p). [e] $E_{LUMO}^{exp} = (E_{HOMO}^{exp} + E_g^{opt})$. [f] E_g^{opt}. Optical energy gap determined from the UV−vis absorptions in solution. [g] E_g^{calcd}, calculated by TD-DFT TD/PBE0/6-311G(d,p)//PBE0/6-311G(d,p) as first excitation energy.

DOI: 10.1021/acs.joc.7b00961
J. Org. Chem. 2017, 82, 6904−6912

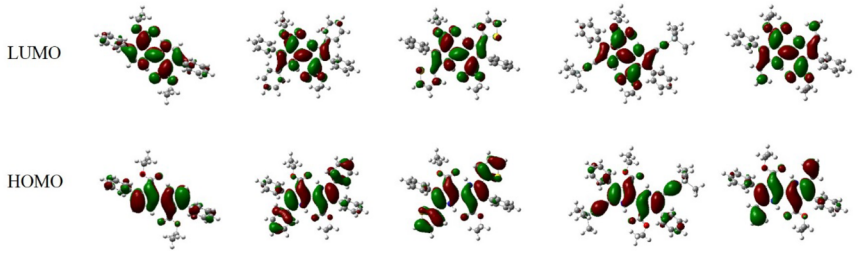

Figure 8. Frontier molecular orbitals of bipyrroles **2a** and **3a–d**.

In general, the calculated bond lengths are in good agreement with the X-ray results. However, the dihedral angles between pyrroles and rings at positions 5,5′ are slightly overestimated. This effect has already been observed in other conjugated systems.[53] Next, the frontier molecular orbitals (FMO) plots and the HOMO and LUMO levels were evaluated by single-point calculations at the B3LYP/6-311G(d,p)//B3LYP/6-311G(d,p) level of theory. The calculated HOMO energy levels of bipyrroles **3** are in reasonably good agreement (±0.2 eV) with the values extracted from the cyclic voltammograms (Table 4). As shown in Figure 8, the HOMO were spread out over the bipyrrole core and the conjugated substituents at positions 5,5′, while the LUMO were mainly localized to the bipyrrole moieties. As expected, the phenyl rings at positions 4,4′, which are not coplanar with the bipyrrole moiety, do not contribute to the delocalization of the FMO (Figure 8).

To gain insight into the electronic transitions of bipyrroles **3**, time-dependent DFT calculations (TD-DFT) were performed in chloroform as solvent. Two different functionals (B3LYP and PBE0)[54] and several basis sets were assessed and compared with the experimental data. The most accurate results were obtained using the TD/PBE0/6-311G(d,p)//PBE0/6-311G(d,p) level of theory.

The results are summarized in Table 5. The calculated absorption maximums, although accurate, are generally red-shifted with respect to the experimental spectra. Moreover, from the first excitation energy the HOMO–LUMO gaps (E_g^{calcd}) were extracted. These calculated values are approximately comparable to the optical HOMO–LUMO gaps (E_g^{exp}) estimated from the corresponding UV–vis spectra (Table 4). According to Musgrave et al.,[55] the expression $E_{LUMO}^{exp} = (E_{HOMO}^{exp} + E_g^{opt})$ was used to calculate the LUMO energy level.

Table 5. UV–vis Spectroscopic Data and Calculated Lowest Excitation Energies of 2a and 3a–d

compd	$\lambda_{max}^{abs,\,exp}$ (nm)	$\lambda_{max}^{abs,calcd}$ (nm)	composition of the band
2a	362	373 (0.81)	H→L (99%)
3a	406, 332	414 (0.75)	H→L (99%)
		337 (0.48)	H→L+1 (92%) H→L+2 (5%)
3b	390, 314	383 (0.77)	H→L (99%)
		311 (0.58)	H→L+2 (96%)
3c	383, 305	394 (0.78)	H→L (99%)
		315 (0.56)	H→L+2 (94%) H→L+1 (2%)
3d	399, 313	404 (0.64)	H→L (99%)
		312 (0.5)	H→L+1 (96%)

The TD-DFT calculations suggest that the lowest energy absorption band for these bipyrroles is mainly contributed by the HOMO → LUMO transition with high oscillator strength above 0.6, which corresponds to the electronic transition from the ground to the first excited state (S0 → S1). On the other hand, the second absorption maximum is related to the mixed HOMO–LUMO+1 or HOMO–LUMO+2 transitions (Table 5, Figure S36).

CONCLUSIONS

5,5′-Dibrominated 2,2′-bipyrroles have been used as starting materials to prepare a new family of 5,5′-substituted 2,2′-bipyrroles. The introduction of thienyl, phenyl, TMS-ethynyl, and vinyl groups was achieved by means of the Stille reaction. The usual reflux conditions for this coupling were advantageously substituted by microwave irradiation. Under these conditions, the time of reaction can be reduced from 48 to 3 h. The crystal structures of four of these bipyrroles reveal that the heterocyclic substituents adopt a planar *trans* configuration. Strikingly, although the phenyl groups are nearly perpendicular to the bipyrrole moiety, rings at positions 5,5′ remain coplanar with the heterocyclic core. As a consequence, the presence of such substituents causes an extension of the π-conjugation, which is in agreement with the observed red-shifting of the bands in the UV–vis spectra. As anticipated, bipyrroles **3** display a strong fluorescence emission around 460 nm with quantum yields ranging from 23% to 77%. The introduction of octyl chains enhances the solubility of these bipyrroles without affecting their optical properties. From thermogravimetric analysis, it can be concluded that these bipyrroles are endowed with high chemical and thermal stability. These properties make them useful for optoelectronic applications, for instance, as monomers to prepare conjugated polymers. Preliminary results point out that reaction of dibrominated bipyrroles **4** and distannylated compounds can be coupled to afford mixed polymers with interesting optical properties. A complete study of these materials is currently ongoing in our laboratories.

EXPERIMENTAL SECTION

General Methods and Materials. All reagents and solvents of analytical grade were purchased directly from commercial sources and used without any further purification. Anhydrous solvents were drawn into syringes under the flow of dry N_2 gas and directly transferred into the reaction flasks to avoid contamination. Column chromatography was carried out on silica gel (70–230 mesh), and analytical thin layer chromatography (TLC) was performed on plastic plates of silica gel GF-254 with detection by UV. Standard techniques for synthesis were carried out under nitrogen atmosphere. All melting points were determined in a Büchi 530 capillary apparatus without any correction. Elemental analyses were performed on a Carlo-Erba CHNS-O/EA 1108 instrument.

Microwave Irradiation. Experiments were performed in an Initiator (Biotage) microwave apparatus, operating at a frequency of 2.45 GHz with continuous irradiation power from 0 to 400 W. Reactions were carried out in 5 and 20 mL glass tubes (Biotage), sealed with aluminum/Teflon crimp tops, which can be exposed up to

DOI: 10.1021/acs.joc.7b00961
J. Org. Chem. 2017, 82, 6904–6912

250 °C and 20 bar internal pressure. The temperature was measured with an IR sensor on the outer surface of the process vial. After the irradiation period, the reaction vessel was cooled rapidly to 50 °C by air jet cooling. For the Stille couplings, the reaction temperature was 140 °C (100 °C/min slope) for 3 h and Suzuki reaction at 120 °C (100 °C/min slope) for 1.5 h.

Spectroscopy and Spectrometry. The absorption and photoluminescence spectra were measured using a double-beam spectrometer (Thermo Scientific 300 UV−vis) and a fluorescence spectrometer (Hitachi F2500), respectively, in chloroform at room temperature (25 °C). Fluorescence spectra were obtained using the corresponding maximum absorption wavelengths as excitation wavelengths in chloroform, and fluorescence quantum yields (Φ_f) were estimated using a H_2SO_4 0.005 M solution of quinine sulfate as a standard with a known value of Φ_F = 0.546 at room temperature. ^{1}H NMR and ^{13}C NMR spectra were recorded in a Varian-400MR spectrometer. Chemical shift values (δ) were reported in parts per million relative to TMS as the internal standard (^{1}H NMR) or to the residual solvent peak (^{13}C NMR). IR spectra were recorded in a Nicolet iS10 FTIR spectrometer. HRMS were recorded using an Agilent Technologies 5975 spectrometer.

High-Resolution Mass Spectrometry. HRMS spectra were recorded on an EBE Trisector VG AutoSpec (Micromass Instruments) high-resolution spectrometer (FAB mode). HR-FAB-MS spectra were recorded with *m*-nitrobenzyl alcohol (NBA) as a matrix.

Electrochemistry. Cyclic voltammograms were recorded on a Voltalab PST050 using a three-electrode single-compartment cell (20 mL) at different scan rates (20, 50, 100 mV/s). 0.5 × 10^{-3} M CH_2Cl_2 solutions containing $TBAClO_4$ (0.1 M) as supporting electrolyte were prepared. The electrodes used were a Pt wire working electrode, a Pt wire counter electrode, and Ag/$AgNO_3$ 0.01 M with 0.1 TBAP (tetrabutylammonium perchlorate) as a reference electrode at room temperature. Prior to each measurement, the solutions were degassed by nitrogen bubbling for 10 min. The ferrocene/ferrocinium (Fc/Fc^+) couple was used as the internal standard in each CV.

Crystallography. Diffraction data were collected on a high flux microfocus Rigaku FRX rotating anode at the copper k_α wavelength equipped with a Dectris Pilatus 200 K hybrid detector. The crystals were mounted on cryo-loops after quick soaking on Paratone-N oil from Hampton research and flash-frozen at 120 and 100 K (structure **3a**). The data were processed with the CrystalClear suite version 2.1 b43.[56] All crystal structures was solved with SHELXT[57] and refined using SHELXL 2014[58] version. Full-matrix least-squares refinement were performed on F^2 for all unique reflections, minimizing $w(F_o^2 - F_c^2)^3$ with anisotropic displacement parameters for non-hydrogen atoms. All H atoms found in difference electron-density maps were refined freely, and all the other were treated as riding on their parent C or N atoms. Data statistics are reported in the CIFs and Table 2. Crystals of bipyrroles **2a** (CCDC 1490137), **3a** (CCDC 1490136), **3b** (CCDC 1490111), and **3f** (CCDC 1487240) contain the supplementary crystallographic data for this paper. These data can be obtained free of charge from the Cambridge Crystallographic Data Centre via www.ccdc.cam.ac.uk/data_request/cif.

Computational Details. The computations were performed using Gaussian 09[59] with a GaussView interface on a computer with a quad-core processor. The geometries were optimized at the DFT B3LYP level of theory with a 6-311G(d,p) basis set.[52] The structures are minima on the potential energy surface with positive harmonic vibrational frequencies.

Synthesis of 4,4′-Diaryl-2,2′-bipyrroles 2a,b. *Typical Procedure.* *n*-BuLi (1.6 M in hexanes, 10.4 mL, 17 mmol) was added to a solution of TosMIC (1.56 g, 8.0 mmol) in tetrahydrofuran (THF) (50 mL) at −78 °C. After 5 min of stirring at −78 °C, 16 mL of Me_3SnCl (1 M in THF, 16 mmol) were added dropwise. After another 5 min of stirring at −78 °C, a solution of **5a,b** (8.0 mmol) in THF (20 mL) was added dropwise. The temperature of the reaction mixture was allowed to rise to room temperature over 30 min, and stirring was continued overnight. To this solution was added 1.9 g of $Cu(NO_3)_2{\cdot}3H_2O$ (8 mmol) in a single portion. The mixture was stirred at room temperature for 40 min. The solvent was removed under reduced pressure, and the residue was dissolved in ethyl acetate. The organic layer was washed with 10% ammonia (3 × 50 mL), water (3 × 50 mL) and brine. The solvent was dried over $MgSO_4$, and the volume of the solution was reduced to 1/3 of the total. The resulting slurry was placed in the refrigerator overnight, and the precipitate was collected by filtration and washed with cold ethyl acetate.

2a (42%, 0.72 g, pale yellow powder). IR (KBr)/cm^{-1}: 3445, 2989, 1657, 1499, 1423, 1187, 795, 761, 699. ^{1}H NMR (400 MHz, $CDCl_3$) δ: 13.42 (br, 2H), 7.35−7.29 (m, 10H), 6.81 (d, J = 2.7 Hz, 2H), 4.10 (q, J = 7.0 Hz, 4H), 0.94 (t, J = 7.0 Hz, 6H). ^{13}C NMR (100.6 MHz, $CDCl_3$) δ: 168.6, 136.7, 129.6, 129.5, 128.9, 127.4, 126.2, 117.8, 109.6, 60.7, 13.4. HRMS (FAB/EBE trisector, NBA, positive) m/z: $[M]^+$ calcd for $C_{26}H_{25}N_2O_4$ 429.1814, found 429.1814. UV−vis λ_{max}/nm (ε/$M^{-1}{\cdot}cm^{-1}$) $CHCl_3$: 362 (1.6 × 10^4). Mp: 188−190 °C.

2b (26%, 0.68 g, pale yellow powder). IR (KBr)/cm^{-1}: 3437, 2957, 1644, 1510, 1440, 1176, 1118, 1018, 832, 800, 680. ^{1}H NMR (400 MHz, $CDCl_3$) δ: 13.31 (s, 2H), 7.24 (d, J = 8.8 Hz, 4H), 6.89 (d, J = 8.8 Hz, 4H), 6.78 (d, J = 2.8 Hz, 2H), 3.99 (t, J = 6.8, Hz, 4H), 3.63 (s, 6H), 1.86−1.76 (m, 4H), 1.53−1.25 (m, 20H), 0.93−0.86 (t, J = 6.8, 6H). ^{13}C NMR (100.6 MHz, $CDCl_3$) δ: 169.4, 157.9, 130.3, 129.73, 128.8, 128.6, 117.9, 113.8, 109.3, 68.2, 51.6, 31.9, 29.57, 29.5, 29.4, 26.3, 22.83, 14.3. UV−vis λ_{max}/nm (ε/$M^{-1}{\cdot}cm^{-1}$) $CHCl_3$: 368 (2.1 × 10^4). Mp: 122−123 °C. Anal. Calcd for $C_{40}H_{52}N_2O_6$: C, 73.14; H, 7.96; N, 4.35. Found: C, 73.45; H, 7.96; N, 4.35.

Synthesis of Dibrominated 4,4′-Diaryl-2,2′-bipyrroles 4a,b. *Typical Procedure.* 4-Diaryl-2,2′-bipyrrole **2a,b** (2.33 mmol) was dissolved in 100 mL of dry THF. Then to the solution was added *N*-bromosuccinimide (NBS) (0.87 g, 4.90 mmol), and the solution was stirred overnight. The solvent was removed under vacuum, and the solid was dissolved in dichloromethane (DCM) and washed with water (3 × 25 mL). $MgSO_4$ was added, the solution was filtered, and the solvent was removed under vacuum. The pure product was obtained by washing the solid with a mixture of ethyl acetate (AcOEt) and cyclohexane (Cy) (1:1) to give yellow powders.

4a (87%, 1.19 g, pale yellow powder). IR (KBr)/cm^{-1}: 3432, 2981, 1652, 1444, 1416, 1186, 1023, 959, 767, 698, 636. ^{1}H NMR (400 MHz, $CDCl_3$) δ: 13.87 (s, 2H), 7.42−7.23 (m, 10H), 4.04 (q, J = 7.2, 14.4 Hz, 4H), 0.82 (t, J = 7.2, 14.4 Hz, 6H). ^{13}C NMR (100.6 MHz, $CDCl_3$) δ: 167.7, 135.5, 130.3, 129.4, 127.7, 127.7, 127.0, 111.6, 101.6, 61.2, 13.3. HRMS (FAB/EBE trisector, NBA, positive) m/z: $[M]^+$ calcd for $C_{26}H_{22}N_2Br_2O_4$ 583.9946, found 583.9969. UV−vis λ_{max}/nm (ε/$M^{-1}{\cdot}cm^{-1}$) $CHCl_3$: 372 (2.0 × 10^4). Mp: 221−222 °C. Anal. Calcd for $C_{26}H_{22}N_2Br_2O_4$: C, 53.27; H, 3.78; N, 4.78. Found: C, 53.16; H, 3.43; N, 4.67.

4b (75%, 1.42 g, pale yellow powder). IR (KBr)/cm^{-1}: 3433, 2924, 2851, 1658, 1503, 1438,, 1178, 1111, 1001, 832. ^{1}H NMR (400 MHz, $CDCl_3$) δ: 13.76 (s, 2H), 7.18 (d, J = 8.7 Hz, 4H), 6.92 (d, J = 8.7 Hz, 4H), 4.00 (t, J = 6.6, 13.2 Hz, 4H), 3.58 (s, 6H), 1.87−1.76 (m, 4H), 1.53−1.28 (m, 20H), 0.94−0.86 (t, J = 6.8 Hz, 6H). ^{13}C NMR (100.6 MHz, $CDCl_3$) δ: 168.3, 158.3, 131.3, 129.36, 127.2, 127.1, 113.7, 111.2, 101.8, 7.14, 5.0, 32.0, 29.58, 3.55, 29.4, 26.3, 22.8, 14.3. UV−vis λ_{max}/nm (ε/$M^{-1}{\cdot}cm^{-1}$) $CHCl_3$: 376 (2.2 × 10^4). Mp: 160−161 °C. Anal. Calcd for $C_{40}H_{50}Br_2N_2O_6$: C, 58.97; H, 6.19; N, 3.44. Found: C, 58.79; H, 5.91; N, 3.48.

Synthesis of 3a−h by Stille Coupling. *Typical Procedure Using Conventional Heating.* Dibrominated bipyrrole **4a,b** (0.34 mmol) and stannylated derivative **6−9** (0.85 mmol) were dissolved in 20 mL of dry toluene. Then the solution was flushed with N_2 for 20 min, and tetrakis(triphenylphosphine)palladium(0) ($Pd(PPh_3)_4$) (0.12 g, 0.1 mmol) was added. The resulting mixture was flushed for an additional 5 min. Finally, the mixture was stirred for 2 days at 100 °C under nitrogen. The mixture was filtered to separate the precipitated catalyst, and the solvent was removed under reduced pressure to obtain a brown oil. The pure product was obtained washing the brown oil with a mixture of AcOEt and Cy (1:1) to give green-yellow powders.

Synthesis of 3a−h by Stille Coupling. *Typical Procedure Using MW.* Compound **4a,b** (0.34 mmol) and stannylated derivative **6−9** (0.85 mmol) were dissolved in 15 mL of dry toluene. Then the solution was flushed with N_2 for 20 min, and $Pd(PPh_3)_4$ (0.12 g, 0.1 mmol) was added. The resulting mixture was flushed for an additional

DOI: 10.1021/acs.joc.7b00961
J. Org. Chem. 2017, 82, 6904−6912

5 min. Finally, the mixture was stirred for 3 h at 140 °C in a microwave instrument. The mixture was filtered to separate the precipitated catalyst, and the solvent was removed under reduced pressure to obtain a brown oil. The product was obtained washing the brown oil a mixture of AcOEt and Cy (1:1) to yield a green-yellow powder.

3a (87%, 175 mg, yellow orange-powder). IR (KBr)/cm^{-1}: 3065, 2979, 1652, 1499, 1442, 1419, 1182, 1068, 908, 847, 792, 769, 696. ^1H NMR (400 MHz, $CDCl_3$) δ: 14.18 (s, 2H), 7.43−7.31 (m, 10H), 7.09 (dd, J = 3.6, 1.2 Hz, 2H), 7.04 (dd, J = 5.1, 1.2 Hz, 2H), 6.93 (dd, J = 5.1, 3.6 Hz, 2H), 4.04 (q, J = 7.1 Hz, 4H), 0.76 (t, J = 7.1 Hz, 6H).^{13}C NMR (100.6 MHz, $CDCl_3$) δ: 168.4, 136.9, 134.4, 131.0, 128.6, 128.1, 127.1, 127.0, 125.6, 124.9, 124.3, 123.2, 112.3, 60.8, 13.3. UV−vis λ_{max}/nm (ε/M^{-1}·cm^{-1}) $CHCl_3$: 332 (1.6 × 104), 406 (1.9 × 104). Mp: >250 °C. Anal. Calcd for $C_{34}H_{28}N_2O_4S_2$: C, 68.90; H, 4.76; N, 4.73; S, 10.82. Found: C, 68.56; H, 4.98; N, 4.71; S, 10.69.

3b (90%, 178 mg, green-yellow powder). IR (KBr)/cm^{-1}: 3431, 3052, 2979, 1648, 1492, 1419, 1182, 1032, 818, 774, 764, 699. ^1H NMR (400 MHz, $CDCl_3$) δ: 13.94 (s, 2H), 7.37−7.13 (m, 20H), 4.04 (q, J = 7.2 Hz, 4H), 0.79 (t, J = 7.2 Hz, 6H). ^{13}C NMR (100.6 MHz, $CDCl_3$) δ: 168.7, 137.5, 132.1, 130.8, 129.1, 128.9, 128.6, 127.9, 126.8, 126.6, 126.6, 125.7, 112.6, 60.8, 13.3. UV−vis λ_{max}/nm (ε/M^{-1}·cm^{-1}) $CHCl_3$: 314 (1.9 × 104), 390 (2.0 × 104). Mp: 235 °C. Anal. Calcd for $C_{38}H_{32}N_2O_4$: C, 78.60; H, 5.55; N, 4.82. Found: C, 78.70; H, 5.69; N, 4.82.

3c (79%, 167 mg, yellow powder). IR (KBr)/cm^{-1}: 3433, 2958, 1656, 1478, 1418, 1180, 1031, 858, 757, 698. ^1H NMR (400 MHz, $CDCl_3$) δ: 13.30 (s, 2H), 7.39−7.26 (m, 10H), 4.10 (q, J = 7.2 Hz, 4H), 0.90 (t, J = 7.2 Hz, 6H), 0.14 (s, 18H). ^{13}C NMR (100.6 MHz, $CDCl_3$) δ: 168.0, 135.2, 134.2, 130.0, 128.2, 127.7, 126.8, 112.9, 111.2, 99.2, 96.1, 61.2, 13.5, −0.1. UV−vis λ_{max}/nm (ε/M^{-1}·cm^{-1}) $CHCl_3$: 305 (1.9 × 104), 383 (2.4 × 104). Mp: 232−233 °C. Anal. Calcd for $C_{36}H_{40}N_2O_4Si_2$: C, 69.64; H, 6.49; N, 4.51. Found: C, 69.76; H, 6.29; N, 4.49.

3d (63%, 103 mg, yellow powder). TBP was used as radical inhibitor during the reaction. IR (KBr)/cm^{-1}: 3434, 2975, 2924, 1661, 1632, 1602, 1476, 1432, 1180, 1023, 986, 908, 773, 700, 645. ^1H NMR (400 MHz, $CDCl_3$) δ: 13.92 (s, 2H), 7.39−7.24 (m, 10H), 6.38 (dd, J = 17.8, 11.3 Hz, 2H), 5.59 (d, J = 17.8 Hz, 2H), 5.13 (d, J = 11.3 Hz, 2H), 4.04 (q, J = 7.1 Hz, 4H), 0.81 (t, J = 7.1 Hz, 6H). ^{13}C NMR (100.6 MHz, $CDCl_3$) δ: 168.5, 136.2, 130.6, 129.1, 128.9, 127.9, 127.5, 126.6, 125.3, 111.6, 111.0, 60.8, 13.4. UV−vis λ_{max}/nm (ε/M^{-1}·cm^{-1}) $CHCl_3$: 313 (1.6 × 10^4), 399 (1.9 × 10^4). Mp: 250 °C dec. Anal. Calcd for $C_{30}H_{28}N_2O_4$: C, 74.98; H, 5.87; N, 5.83. Found: C, 75.09; H, 5.89; N, 5.84.

3e (90%, 251 mg, yellow-orange powder). IR (KBr)/cm^{-1}: 3435, 2926, 2854, 1656, 1521, 1447, 1397, 1243, 1201, 1172, 830, 687. ^1H NMR (400 MHz, $CDCl_3$) δ: 14.07 (s, 2H), 7.21 (d, J = 8.6 Hz, 4H), 7.11 (dd, J = 3.7, 1.2 Hz, 2H), 7.06 (dd, J = 5.1, 1.2 Hz, 2H), 6.97−6.92 (m, 6H), 4.03 (t, J = 6.7 Hz, 4H), 3.56 (s, 6H), 1.84 (m, 4H), 1.53−1.29 (m, 20H), 0.90 (s, J = 6,7 Hz, 6H). ^{13}C NMR (100.6 MHz, $CDCl_3$) δ: 169.0, 158.6, 134.4, 131.9, 128.6, 128.4, 126.9, 125.2, 125.2, 124.3, 123.1, 114.1, 112.2, 68.2, 51.9, 32.0, 29.6, 29.6, 29.4, 26.3, 22.8, 14.3. Anal. Calcd for $C_{48}H_{56}N_2O_6S_2$: C, 70.21; H, 6.87; N, 3.41; S, 7.81. Found: C, 70.022; H, 7.16; N, 3.27; S, 8.05. UV−vis λ_{max}/nm (ε/M^{-1}·cm^{-1}) $CHCl_3$: 334 (1.8 × 10^4), 408 (2.2 × 10^4). Mp: 212−215 °C.

3f (92%, 253 mg, green-yellow powder). IR (KBr)/cm^{-1}: 3434, 2925, 2855, 1658, 1518, 1444, 1399, 1232, 1200, 1173, 1020, 833, 768, 695. ^1H NMR (400 MHz, $CDCl_3$) δ: 13.80 (s, 2H), 7.32−7.16 (m, 10H), 7,16 (d, J = 8.6 Hz, 4H) 6.88 (d, J = 8.6 Hz, 4H), 4.00 (t, J = 6.6 Hz, 4H), 3.57 (s, 6H), 1.88−1.77 (m, 4H), 1.54−1.28 (m, 20H), 0.95−0.85 (t, J = 6.6 Hz, 6H). ^{13}C NMR (100.6 MHz, $CDCl_3$) δ: 169.1, 157.8, 132.0, 131.5, 129.1, 128.9, 128.6, 128.48, 126.6, 125.0, 113.8, 112.1, 68.0, 51.6, 31.8, 29.4, 29.4, 29.3, 26.9, 26.1, 22.7, 14.1. UV−vis λ_{max}/nm (ε/M^{-1}·cm^{-1}) $CHCl_3$: 314 (1.9 × 10^4), 392 (2.1 × 10^4). Mp: 176−177 °C. Anal. Calcd for $C_{52}H_{60}N_2O_6$: C, 77.20; H, 7.48; N, 3.46. Found: C, 77.38; H, 7.60; N, 3.22.

3g (32%, 92 mg, yellow powder). IR (KBr)/cm^{-1}: 3434, 2923, 2855, 2154, 1657, 1516, 1439, 1385, 1164, 1042, 860, 831. ^1H NMR (400 MHz, $CDCl_3$) δ: 13.15 (s, 2H), 7.30 (d, J = 8.7 Hz, 4H), 6.89 (d, J = 8.7 Hz, 4H), 4.00 (t, J = 6.6 Hz, 4H), 3.64 (s, 6H), 1.86−1.76 (m, 4H), 1.51−1.27 (m, 20H), 0.90 (t, J = 6.8 Hz, 6H), 0.17 (s, 18H). ^{13}C NMR (100.6 MHz, $CDCl_3$) δ: 168.7, 158.2, 133.5, 130.9, 128.1, 126.9, 113.6, 112.7, 110.7, 99.2, 96.3, 68.2, 51.9, 31.9, 29.6, 29.5, 29.4, 26.3, 22.8, 14.3, −0.1. UV−vis λ_{max}/nm (ε/M^{-1}·cm^{-1}) $CHCl_3$: 257 (2.9 × 10^4), 388 (2.1 × 10^4). Mp: 175−176 °C. Anal. Calcd for $C_{50}H_{68}N_2O_6Si_2$: C, 70.71; H, 8.07; N, 3.30. Found: C, 70.44; H, 8.15; N, 3.31.

3h (46%, 113 mg, yellow powder). TBP was used as radical inhibitor during the reaction. IR (KBr)/cm^{-1}: 3456, 2925, 2855, 1657, 1516, 1440, 1391, 1242, 1195, 1163, 833. ^1H NMR (400 MHz, $CDCl_3$) δ: 13.83 (s, 2H), 7.16 (d, J = 8.7 Hz, 4H), 6.91 (d, J = 8.7 Hz, 4H), 6.41 (dd, J = 17.8, 11.3 Hz, 2H), 5.60 (d, J = 17.8 Hz, 2H), 5.14 (d, J = 11.3 Hz, 2H), 4.01 (t, J = 6.6 Hz, 4H), 3.58 (s, 6H), 1.82 (m, 4H), 1.52−1.29 (m, 20H), 0.95−0.86 (t, J = 6.8 Hz 6H). ^{13}C NMR (100.6 MHz, $CDCl_3$) δ: 169.1, 158.0, 131.5, 129.1, 128.9, 127.9, 127.5, 125.5, 113.6, 111.3, 110.9, 68.2, 51.7, 32.0, 29.6, 29.6, 3.4, 26.3, 22.8, 14.3. UV−vis λ_{max}/nm (ε/M^{-1}·cm^{-1}) $CHCl_3$: 313 (1.6 × 10^4), 402 (1.9 × 10^4). Mp: 250 °C(dec. Anal. Calcd for $C_{44}H_{56}N_2O_6$: C, 74.55; H, 7.96; N, 3.95. Found: C, 74.16; H, 8.11; N, 3.91.

Synthesis of 5b by Suzuki Coupling. *Typical Procedure Using MW.* Compound **4a** (0.34 mmol) and boronic derivative **10** (0.85 mmol) were dissolved in 17 mL of DMF. Then the solution was flushed with N_2 for 20 min, and 1,1′-bis(diphenylphosphino)-ferrocene)palladium(II) dichloride ($PdCl_2$(dppf)) (0.075 g, 0.1 mmol) was added. The resulting mixture was flushed for an additional 5 min. Subsequently, a solution of 3 mL of degassed Na_2CO_3 2 M was added, and the mixture was stirred for 1.5 h at 120 °C in a microwave instrument. The solvent was removed under vacuum, and the solid was redissolved in DCM and washed with saturated lithium chloride (5 × 20 mL). $MgSO_4$ was added, the solution was filtered, and the solvent was removed under vacuum. The product was obtained by washing the brown oil with mixtures of AcOEt and Cy to yield a green-yellow powder.

3b (35%, 69 mg, green yellow-powder). ^1H NMR (400 MHz, $CDCl_3$) δ: 13.94 (s, 1H), 7.37−7.13 (m, 10H), 4.04 (q, J = 7.2 Hz, 2H), 0.79 (t, J = 7.2 Hz, 3H). ^{13}C NMR (100.6 MHz, $CDCl_3$) δ: 168.7, 137.5, 132.1, 130.8, 129.1, 128.9, 128.6, 127.9, 126.8, 126.6, 126.6, 125.7, 112.6, 60.8, 13.3.

■ ASSOCIATED CONTENT

Supporting Information

The Supporting Information is available free of charge on the ACS Publications website at DOI: 10.1021/acs.joc.7b00961.

^1H and ^{13}C NMR spectra of all previously unidentified compounds, absorption and fluorescence spectra, cyclic voltammograms, X-ray crystallography information (thermal ellipsoid plots and crystal packing figures), and theoretical data (PDF)

X-ray data for compound **2a** (CIF)

X-ray data for compound **3a** (CIF)

X-ray data for compound **3b** (CIF)

X-ray data for compound **3f** (CIF)

■ AUTHOR INFORMATION

Corresponding Author

*E-mail: david.sanchez@iqs.edu.

ORCID

Salvador Borrós: 0000-0002-4003-0381

David Sánchez-García: 0000-0002-3936-9329

Notes

The authors declare no competing financial interest.

DOI: 10.1021/acs.joc.7b00961
J. Org. Chem. 2017, 82, 6904−6912

■ ACKNOWLEDGMENTS

This work was supported by a grant of the Obra Social "La Caixa" (2016-URL-IR2Q-023). G.A. thanks the Generalitat de Catalunya (DURSI) and the European Social Fund for a predoctoral fellowship (2014FI_B200140).

■ REFERENCES

(1) Rapoport, H.; Castagnoli, N. *J. Am. Chem. Soc.* **1962**, *84*, 2178.
(2) Rapoport, H.; Holden, K. G. *J. Am. Chem. Soc.* **1962**, *84*, 635.
(3) Bonnett, R.; Cannon, J. R.; Clark, V. M.; Johnson, A. W.; Parker, L. F. J.; Smith, E. L.; Todd, A. *J. Chem. Soc.* **1957**, 1158.
(4) Setsune, J.-i. *Chem. Rev.* **2017**, *117*, 3044.
(5) Vogel, E.; Köcher, M.; Schmickler, H.; Lex, J. *Angew. Chem., Int. Ed. Engl.* **1986**, *25*, 257.
(6) Bauer, V. J.; Clive, D. L. J.; Dolphin, D.; Paine, J. B.; Harris, F. L.; King, M. M.; Loder, J.; Wang, S. W. C.; Woodward, R. B. *J. Am. Chem. Soc.* **1983**, *105*, 6429.
(7) Seidel, D.; Lynch, V.; Sessler, J. L. *Angew. Chem., Int. Ed.* **2002**, *41*, 1422.
(8) Nadeau, J. M.; Swager, T. M. *Tetrahedron* **2004**, *60*, 7141.
(9) Merz, A.; Anikin, S.; Lieser, B.; Heinze, J.; John, H. *Chem. - Eur. J.* **2003**, *9*, 449.
(10) Roznyatovskiy, V. V.; Roznyatovskaya, N. V.; Weyrauch, H.; Pinkwart, K.; Tubke, J.; Sessler, J. L. *J. Org. Chem.* **2010**, *75*, 8355.
(11) Groenendaal, L.; Peerlings, H. W. I.; van Dongen, J. L. J.; Havinga, E. E.; Vekemans, J. A. J. M.; Meijer, E. W. *Macromolecules* **1995**, *28*, 116.
(12) Tshibaka, T.; Bishop, S.; Roche, I. U.; Dufresne, S.; Lubell, W. D.; Skene, W. G. *Chem. - Eur. J.* **2011**, *17*, 10879.
(13) Grigg, R.; Johnson, A. W.; Wasley, J. W. F. *J. Chem. Soc.* **1963**, 359.
(14) van Haare, J. A. E. H.; Groenendaal, L.; Peerlings, H. W. I.; Havinga, E. E.; Vekemans, J. A. J. M.; Janssen, R. A. J.; Meijer, E. W. *Chem. Mater.* **1995**, *7*, 1984.
(15) Groenendaal, L.; Bruining, M. J.; Hendrickx, E. H. J.; Persoons, A.; Vekemans, J. A. J. M.; Havinga, E. E.; Meijer, E. W. *Chem. Mater.* **1998**, *10*, 226.
(16) Andrieux, C. P.; Hapiot, P.; Audebert, P.; Guyard, L.; Dinh An, M. N.; Groenendaal, L.; Meijer, E. W. *Chem. Mater.* **1997**, *9*, 723.
(17) Sánchez-García, D.; Borrell, J. I.; Nonell, S. *Org. Lett.* **2009**, *11*, 77.
(18) Anguera, G.; Kauffmann, B.; Borrell, J. I.; Borros, S.; Sánchez-García, D. *Org. Lett.* **2015**, *17*, 2194.
(19) Zhang, K.; Savage, M.; Li, X.; Jiang, Y.; Ishida, M.; Mitsuno, K.; Karasawa, S.; Kato, T.; Zhu, W.; Yang, S.; Furuta, H.; Xie, Y. *Chem. Commun.* **2016**, *52*, 5148.
(20) Kong, J.; Li, Q.; Li, M.; Li, X.; Liang, X.; Zhu, W.; Ågren, H.; Xie, Y. *Dyes Pigm.* **2017**, *137*, 430.
(21) Kong, J.; Zhang, Q.; Savage, M.; Li, M.; Li, X.; Yang, S.; Liang, X.; Zhu, W.; Ågren, H.; Xie, Y. *Org. Lett.* **2016**, *18*, 5046.
(22) Ding, Y.; Tang, Y.; Zhu, W.; Xie, Y. *Chem. Soc. Rev.* **2015**, *44*, 1101.
(23) Hong, T.; Song, H.; Li, X.; Zhang, W.; Xie, Y. *RSC Adv.* **2014**, *4*, 6133.
(24) Anguera, G.; Borros, S.; Borrell, J. I.; Sánchez-García, D. *J. Porphyrins Phthalocyanines* **2016**, *20*, 1055.
(25) Zhang, Z.; Cha, W. Y.; Williams, N. J.; Rush, E. L.; Ishida, M.; Lynch, V. M.; Kim, D.; Sessler, J. L. *J. Am. Chem. Soc.* **2014**, *136*, 7591.
(26) Oohora, K.; Ogawa, A.; Fukuda, T.; Onoda, A.; Hasegawa, J. Y.; Hayashi, T. *Angew. Chem., Int. Ed.* **2015**, *54*, 6227.
(27) Ding, Y.; Zhu, W. H.; Xie, Y. *Chem. Rev.* **2017**, *117*, 2203.
(28) Sumrak, J. C.; Sokolov, A. N.; MacGillivray, L. R. *Self-Organized Organic Semiconductors*; Wiley: Hoboken, 2010.
(29) Sun, M.; Wang, L.; Yang, W. *J. Appl. Polym. Sci.* **2010**, *118*, 1462.
(30) Pfaff, U.; Hildebrandt, A.; Schaarschmidt, D.; Rüffer, T.; Low, P. J.; Lang, H. *Organometallics* **2013**, *32*, 6106.
(31) van Mullekom, H. A. M.; Vekemans, J. A. J. M.; Meijer, E. W. *Chem. - Eur. J.* **1998**, *4*, 1235.
(32) van Mullekom, H. A. M.; Venkemans, J. A. J. M.; Meijer, E. W. *Chem. Commun.* **1996**, 2163.
(33) Edder, C.; Armstrong, P. B.; Prado, K. B.; Frechet, J. M. *Chem. Commun.* **2006**, 1965.
(34) Sotzing, G. A.; Reynolds, J. R.; Katritzky, A. R.; Soloducho, J.; Belyakov, S.; Musgrave, R. *Macromolecules* **1996**, *29*, 1679.
(35) Wu, C. Y.; Chen, M. S.; Lin, C. A.; Lin, S. C.; Sun, S. S. *Chem. - Eur. J.* **2006**, *12*, 2263.
(36) McQuade, D. T.; Pullen, A. E.; Swager, T. M. *Chem. Rev.* **2000**, *100*, 2537.
(37) Thomas, S. W.; Joly, G. D.; Swager, T. M. *Chem. Rev.* **2007**, *107*, 1339.
(38) Anzenbacher, P., Jr; Jursikova, K.; Aldakov, D.; Marquez, M.; Pohl, R. *Tetrahedron* **2004**, *60*, 11163.
(39) Zhang, S.; Lv, G.; Wang, G.; Zhu, K.; Yu, D.; Shao, J.; Wang, Y.; Liu, Y. *J. Photochem. Photobiol., A* **2015**, *309*, 30.
(40) Hassan, J.; Sévignon, M.; Gozzi, C.; Schulz, E.; Lemaire, M. *Chem. Rev.* **2002**, *102*, 1359.
(41) Banwell, M. G.; Goodwin, T. E.; Ng, S.; Smith, J. A.; Wong, D. J. *Eur. J. Org. Chem.* **2006**, *2006*, 3043.
(42) Larhed, M.; Moberg, C.; Hallberg, A. *Acc. Chem. Res.* **2002**, *35*, 717.
(43) Blettner, C. G.; König, W. A.; Stenzel, W.; Schotten, T. *J. Org. Chem.* **1999**, *64*, 3885.
(44) Handy, S. T.; Bregman, H.; Lewis, J.; Zhang, X.; Zhang, Y. *Tetrahedron Lett.* **2003**, *44*, 427.
(45) Okawara, T.; Doi, A.; Ono, T.; Abe, M.; Takehara, K.; Hisaeda, Y.; Matsushima, S. *Tetrahedron Lett.* **2015**, *56*, 1407.
(46) Sarma, M.; Chatterjee, T.; Ghanta, S.; Das, S. K. *J. Org. Chem.* **2012**, *77*, 432.
(47) Che, C.-M.; Wan, C.-W.; Lin, W.-Z.; Yu, W.-Y.; Zhou, Z.-Y.; Lai, W. Y.; Lee, S. T. *Chem. Commun.* **2001**, 721.
(48) Chi, C.; Wegner, G. *Macromol. Rapid Commun.* **2005**, *26*, 1532.
(49) E, W.; Ohkubo, K.; Sánchez-García, D.; Zhang, M.; Sessler, J. L.; Fukuzumi, S.; Kadish, K. M. *J. Phys. Chem. B* **2007**, *111*, 4320.
(50) Zhang, M.; E, W.; Ohkubo, K.; Sánchez-García, D.; Yoon, D.-W.; Sessler, J. L.; Fukuzumi, S.; Kadish, K. M. *J. Phys. Chem. A* **2008**, *112*, 1633.
(51) Becke, A. D. *J. Chem. Phys.* **1993**, *98*, 1372.
(52) Becke, A. D. *J. Chem. Phys.* **1993**, *98*, 5648.
(53) Kato, S.; Shimizu, S.; Kobayashi, A.; Yoshihara, T.; Tobita, S.; Nakamura, Y. *J. Org. Chem.* **2014**, *79*, 618.
(54) Adamo, C.; Jacquemin, D. *Chem. Soc. Rev.* **2013**, *42*, 845.
(55) Zhang, G.; Musgrave, C. B. *J. Phys. Chem. A* **2007**, *111*, 1554.
(56) *Rigaku CrystalClear-SM Expert 2.1 b43*; Rigaku Americas Corp.: The Woodlands, Texas, 2015.
(57) Sheldrick, G. M. *Acta Crystallogr., Sect. A: Found. Adv.* **2015**, *71*, 3.
(58) Sheldrick, G. M. *Acta Crystallogr., Sect. C: Struct. Chem.* **2015**, *71*, 3.
(59) Frisch, M. J.; Trucks, G. W.; Schlegel, H. B.; Scuseria, G. E.; Robb, M. A.; Cheeseman, J. R.; Scalmani, G.; Barone, V.; Mennucci, B.; Petersson, G. A.; Nakatsuji, H.; Caricato, M.; Li, X.; Hratchian, H. P.; Izmaylov, A. F.; Zheng, G.; Sonnenberg, J. L.; Hada, M.; Ehara, M.; Toyota, K.; Fukuda, R.; Hasegawa, J.; Ishida, M.; Nakajima, T.; Honda, Y.; Kitao, O.; Nakai, H.; Vreven, T.; Montgomery, J. A., Jr.; Peralta, J. E.; Ogliaro, F.; Bearpark, M.; Heyd, J. J.; Brothers, E.; Kudin, K. N.; Staroverov, V. N.; Kobayashi, R.; Normand, J.; Raghavachari, K.; Rendell, A.; Burant, J. C.; Iyengar, S. S.; Tomasi, J.; Cossi, M.; Rega, N.; Millam, N. J.; Klene, M.; Knox, J. E.; Cross, J. B.; Bakken, V.; Adamo, C.; Jaramillo, J.; Gomperts, R.; Stratmann, R. E.; Yazyev, O.; Austin, A. J.; Cammi, R.; Pomelli, C.; Ochterski, J. W.; Martin, R. L.; Morokuma, K.; Zakrzewski, V. G.; Voth, G. A.; Salvador, P.; Dannenberg, J. J.; Dapprich, S.; Daniels, A. D.; Farkas, Ö.; Foresman, J. B.; Ortiz, J. V.; Cioslowski, J.; Fox, D. J. *Gaussian 09*; Gaussian, Inc.: Wallingford, CT, 2009.

DOI: 10.1021/acs.joc.7b00961
J. Org. Chem. 2017, 82, 6904−6912